

Continuum-statistical dynamics of colloidal suspensions under kinematic reversibility

Jerome Burelbach¹

¹International School Michel Lucius, 157 avenue Pasteur, 2311 Luxembourg, Luxembourg

June 2, 2026

Abstract

We present a linear response theory that establishes the continuum-mechanical origin of Onsager reciprocity in colloidal motion. By decoupling hydrostatic and hydrodynamic stress, we show that Onsager reciprocal relations emerge when the Lorentz reciprocal theorem is applied under kinematic reversibility to the auxiliary flow problem of colloidal sedimentation. Our framework applies to suspensions containing multiple species of microparticles and derives all non-equilibrium contributions to colloidal diffusion from a single application of the Lorentz reciprocal theorem, irrespective of whether a slip or no-slip hydrodynamic boundary condition is imposed at the colloidal surface. Furthermore, a boundary-layer treatment is only assumed for ciliary motion, while the hydrostatic forces giving rise to non-equilibrium thermodynamic motion are fully resolved beyond the boundary-layer approximation. In particular, our framework is consistent with classical osmosis through a semi-permeable membrane, where fluid flow occurs without interfacial potential interactions. For diffusiophoresis due to volume exclusion of a solute, our results therefore predict colloidal motion towards higher solute concentration for thin excluded-volume layers, whereas the opposite trend is recovered for longer-ranged, moderately repulsive potentials.

1 Introduction

Continuum mechanics describes a multicomponent system in terms of continuous media that meet at well-defined boundaries, by partitioning the system into a fine mesh of elementary volumes of size dV , each of which is homogeneous in the thermodynamic limit. Once the continuum scale of dV is identified, the dynamics is governed by conservation laws in the form of differential continuity equations for mass, particle number, momentum and energy, expressed in terms of fluxes and source densities defined throughout these media. These continuity equations are closed by assuming that each elementary volume is in local thermodynamic equilibrium (LTE), yielding linear constitutive relations between fluxes and gradients of certain thermodynamic and hydrodynamic continuum fields.[1] Within Onsager's theory of non-equilibrium thermodynamics, time-reversal symmetry implies that the transport coefficients in these relations are symmetric, a result known as the Onsager reciprocal relations.[2, 3] However, in non-equilibrium thermodynamics these coefficients are phenomenological quantities, dependent on molecular correlations and therefore only inferable from experiments or from molecular-dynamics simulations. This poses a limitation for describing the dynamics in colloidal suspensions, where molecular-level modelling is impractical.

To overcome this limitation, Derjaguin modelled the constituent particles of a medium as continuous objects on their own, thus obtaining continuum-mechanical expressions of transport coefficients based on

Onsager reciprocal symmetry.[4] This approach reduces the phenomenological character of coupling in the low Knudsen number regime, where the molecular effect on transport is captured by well-defined boundary conditions. However, since the underlying continuity equations are generally not time-reversible, such Onsager reciprocal approaches effectively postulate reciprocal symmetry at the continuum scale without clarifying the solvent's role in momentum relaxation.[5, 6] From a continuum-mechanical perspective, such a reciprocal symmetry is justified by the principle of kinematic reversibility, which is a prerequisite for applying the Lorentz reciprocal theorem (LRT). In contrast, continuum-mechanical reciprocal approaches often treat the underlying driving forces phenomenologically within a boundary-layer approximation (BLA), based on an effective slip velocity[7] or interfacial tension gradient,[8] despite the fact that these may be related to thermodynamic equations of state. Indeed, an accurate prediction of phoretic mobilities relies on fully resolving the coupling between thermodynamic forces and hydrodynamic flows beyond the BLA, especially when the colloidal radius is comparable to the interfacial layer thickness.[9] Hence, reducing the phenomenological character of colloidal transport remains a fruitful area of active research, as evidenced by recent applications of the LRT, which often focus on force-free transport of a single colloid while assuming a no-slip hydrodynamic boundary condition at its surface.[10, 11, 12, 13]

2 Summary of results

Here, we demonstrate that the aforementioned restrictions are unnecessary when the LRT is applied to a representative volume element of the suspension, rather than the fluid region alone, based on the auxiliary flow problem of colloidal sedimentation. Our approach provides a clear perspective on the underlying assumptions of kinematic reversibility, the solvent's role in momentum relaxation, and the driving forces governing diffusion and advection in colloidal suspensions.

In particular, we generalise the boundary-layer result for the swimming velocity \mathbf{v}_{swim} due to ciliary motion to arbitrary hydrodynamic slippage. The result is given by

$$\mathbf{v}_{\text{swim}} = -\frac{\langle \mathbf{u}_a \rangle_{\partial\nu_c}}{1 + 2l_{\text{slip}}}, \quad (1)$$

where l_{slip} is the hydrodynamic slip length and $\langle \mathbf{u}_a \rangle_{\partial\nu_c}$ is the surface average of the active slip velocity \mathbf{u}_a at the colloidal surface $\partial\nu_c$.

We also show that the diffusio-phoretic velocity \mathbf{v}_Δ of a colloid due to exclusion of an ideal solute from a region of radius $R + \lambda$ around its hydrodynamic centre takes the form

$$\mathbf{v}_\Delta = -\frac{R^2}{9s\eta} \left[x [2x^2 + 3(2-s)x + 6(1-s)] - \frac{1}{2} (3sx^2 + 6sx + 2) \right] k_B T \nabla n_k^b, \quad (2)$$

where $x = \lambda/R$ and η is the viscosity of the solution. The hydrodynamic slip parameter $s = (1 + 2l_{\text{slip}}/R)/(1 + 3l_{\text{slip}}/R)$ takes the value 1 for a no-slip boundary condition and 2/3 for a perfect-slip boundary condition. The bulk osmotic pressure gradient is given by $k_B T \nabla n_k^b$, where T is the temperature, k_B is the Boltzmann constant and n_k^b is the solute number density imposed in the bulk of the solution. In contrast to Anderson's classical result,[7] this expression yields a zeroth-order contribution in the BLA ($x \ll 1$) that drives the colloid towards higher bulk solute concentration, given by

$$\mathbf{v}_\Delta = \frac{R^2}{9s\eta} k_B T \nabla n_k^b. \quad (3)$$

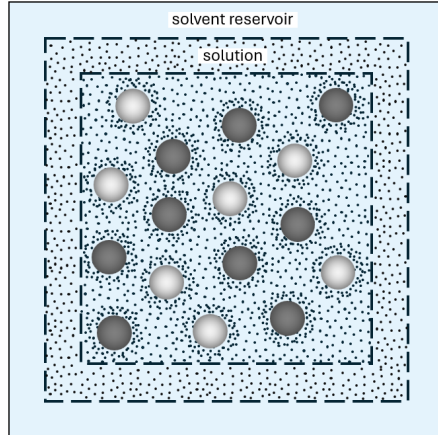


Figure 1: Schematic representation of a suspension. The dark and light gray spheres represent different species of microparticles, consisting of different solid microphases and suspended in a solution. The solution consists of small solutes (black dots) dispersed in a solvent reservoir (light blue background). If the dark gray spheres are the colloids, then the fluid comprises the solution and the light gray spheres. The dashed lines represent thermodynamic reservoir boundaries.

Under the same bulk conditions, an isotropic diffusion-limited absorption of solute particles at the surface of a chemically active colloid instead yields

$$\mathbf{v}_\Delta = -\frac{2R^2}{9s\eta}k_B T \nabla n_k^b, \quad (4)$$

which corresponds to diffusiophoresis towards lower bulk solute concentration.

More generally, we demonstrate that continuum-mechanical Onsager reciprocal relations in colloidal motion emerge directly from the symmetry of the LRT, provided that hydrostatic and hydrodynamic stresses are carefully decoupled within a suspension at local thermodynamic equilibrium.

3 Definitions and assumptions

The system under consideration is a volume-filling, incompressible colloidal suspension, which may include chemical or thermal sources, but must conserve mass internally. We focus our discussion on translational motion and assume that magnetic fields are absent. The local dynamics is described continuum-mechanically at a microscopic scale, relative to an inertial laboratory frame. At this scale, we refer to a collection of indistinguishable particles of a given chemical species as a component of the suspension, and introduce a microphase as a continuous medium composed of a combination of such components. As shown in Fig. 1, the suspension consists of different species of microparticles and small solutes dispersed in a solvent reservoir, such that within a macroscopic representative volume element \mathcal{V} of volume $V = L^3$, we have $N_c \ll N_k \ll N_l$, where N_c , N_k and N_l are the number of particles of any microparticle species c , solute component k , and solvent component l , respectively.

The solvent and the small solutes suspended in it constitute an isotropic viscous microphase (" η ") referred to as the solution, occupying a partial region ν_η within \mathcal{V} , whereas the microparticles ("m") occupy a partial

region $\nu_m = \mathcal{V} \setminus \nu_\eta$ of volume V_m . Each microparticle species consists of a solid microphase, made of chemically bound components that do not support viscous shear or diffusion. The solution meets the surfaces of the microparticles at well-defined interfacial boundaries, where it remains isotropic assuming that molecular crowding and orientational correlations can be ignored. At such a boundary, we distinguish between interfacial body forces, which derive from potential gradients, and interfacial collisional interactions, which are mapped onto corresponding boundary conditions. The colloids ("c") are a chosen species of microparticles whose motion we seek to determine, specified by a given index value c and occupying a partial region ν_c of volume V_c , such that $\nu_m = \bigcap_c \nu_c$ and $V_m = \sum_c V_c$. The fluid ("~") refers to the surrounding solution and all other microparticle species suspended in it, excluding the colloids and thus occupying a partial region $\tilde{\nu} = \mathcal{V} \setminus \nu_c$.

The principle of kinematic reversibility is based on a low Knudsen number, low Reynolds number, and low Mach number, which are all tied to the solvent's role in momentum relaxation. The solvent is therefore modelled as a strongly coupled, viscous, molecular medium, rapidly responding to non-equilibrium forces to maintain a local mechanical equilibrium under the constraint of incompressible flow. Additionally, kinematic reversibility requires that the coupling between flows and forces within the same region occurs under the same dynamic viscosity and component number densities. This requirement, which is essential for a linear-response theory based on the symmetry encoded in the Lorentz reciprocal theorem, does not imply spatial uniformity of the coupling coefficients, but rather that they remain unchanged under different force fields. The condition of LTE must therefore hold not only at the continuum scale of dV , but also at the macroscopic scale of a representative volume element \mathcal{V} of the suspension, which is therefore treated as statistically homogeneous. In the dilute limit, when all microparticle species are present at low volume fractions, the diffusion of a single colloid suspended in an unbounded solution is then recovered. This condition of representative thermodynamic equilibrium (RTE) justifies a decomposition into hydrostatic and hydrodynamic stress and implies that the hydrostatic forces induced by the colloids derive from a thermodynamic equation of state. In addition, RTE ensures that the macroscopic suspension dynamics is slow compared to the relaxation dynamics of local continuum fields. As a result, local continuity equations can be solved at quasi-steady-state under slowly evolving boundary conditions determined by the macroscopic evolution of the suspension. In what follows, the term "first order" will be used to refer to quantities evaluated to first order in the forces that arise from non-equilibrium boundary conditions. In contrast to an elementary volume at LTE, there is no requirement for these forces to remain spatially uniform within a representative volume element at RTE. Equilibrium quantities, which are considered to zeroth order in the non-equilibrium forces, are denoted by a superscript "eq".

4 Disturbance fields and continuity equations

Describing the motion of every individual colloid in a suspension of multiple species of microparticles is a challenging many-body interaction problem. However, many industrial applications are not concerned with the motion of each colloid, but rather with the average dynamics of an ensemble of colloids. Therefore, we seek a macroscopic, continuum-statistical description of colloidal motion, which involves two distinct types of disturbance fields.

On one hand, force-free phoretic motion stems from continuum-mechanical disturbances induced by the colloids relative to the bulk fluid ("b"), which corresponds to the hypothetical reference state of a representative volume element \mathcal{V} obtained by replacing the colloids inside \mathcal{V} by fluid. The disturbance of a field \mathbf{q} induced by the colloids relative to the bulk fluid is defined by

$$\delta \mathbf{q} = \mathbf{q} - \mathbf{q}^b, \quad (5)$$

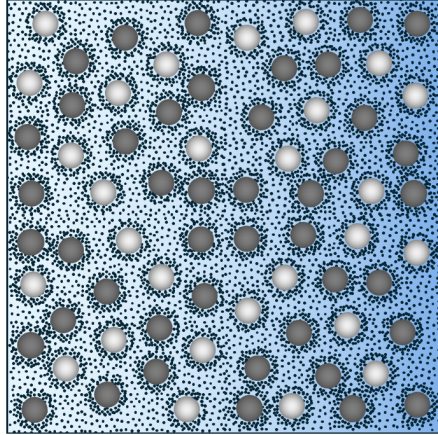


Figure 2: A representative volume element of a homogeneous suspension. The blue background gradient shows that the volume element is subjected to forces due to non-equilibrium boundary conditions.

where \mathbf{q}^b is the field of the bulk fluid, defined everywhere inside \mathcal{V} . Based on Eq. (5), we also have $\delta \nabla \cdot \mathbf{q} = \nabla \cdot \delta \mathbf{q}$ and $\delta (g\mathbf{q}) = \delta g\mathbf{q} + g^b \delta \mathbf{q}$, where g is a scalar. On the other hand, colloidal diffusion is described as a disturbance relative to the average motion, or advection, of the suspension. Unlike diffusion in molecular mixtures, however, which is described relative to the barycentric reference frame,[1] the natural reference frame for colloidal diffusion is the frame of zero mean volume flux, since macroscopic continuity equations can be obtained by averaging over a representative volume element \mathcal{V} of a homogeneous suspension.[14, 15] To this end, the system is divided into a mesh of such volume elements, each of size V . For a given volume element \mathcal{V} , which is illustrated in Fig. 2, let ν_α denote the partial region of volume V_α occupied by a homogeneous medium α . Within \mathcal{V} , the ensemble average, or mean-field, of \mathbf{q} over this medium is then equal to the volume average over its partial region ν_α ,[15] given by $\langle \mathbf{q} \rangle_{\nu_\alpha} = V_\alpha^{-1} \int_{\nu_\alpha} \mathbf{q} d^3\mathbf{r}$, where $\langle \mathbf{q} \rangle_{\nu_\alpha}$ is a uniform field defined everywhere inside \mathcal{V} . The disturbance of \mathbf{q} relative to $\langle \mathbf{q} \rangle_{\nu_\alpha}$ is then defined as

$$\mathbf{q}'_{\nu_\alpha} = \mathbf{q} - \langle \mathbf{q} \rangle_{\nu_\alpha}, \quad (6)$$

such that $\langle \mathbf{q}'_{\nu_\alpha} \rangle_{\nu_\alpha} = 0$. If \mathbf{q} is a flux whose normal component is continuous across all boundaries inside ν_α , we can further write $\langle \nabla \cdot \mathbf{q} \rangle_{\nu_\alpha} = \bar{\nabla} \cdot \langle \mathbf{q} \rangle_{\nu_\alpha}$, where $\bar{\nabla}$ denotes the macroscopic gradient over adjacent volume elements. The average over a representative volume element, or suspension average, is written as

$$\langle \mathbf{q} \rangle = \frac{1}{V} \int_{\mathcal{V}} \mathbf{q} d^3\mathbf{r}, \quad (7)$$

and defines the macroscopic field of \mathbf{q} , which can also be expressed in terms of partial volume averages as $\langle \mathbf{q} \rangle = \gamma_\alpha \langle \mathbf{q} \rangle_{\nu_\alpha} + (1 - \gamma_\alpha) \langle \mathbf{q} \rangle_{\mathcal{V} \setminus \nu_\alpha}$, where $\gamma_\alpha = V_\alpha/V$ is the volume fraction of medium α and $\langle \mathbf{q} \rangle_{\mathcal{V} \setminus \nu_\alpha}$ is the volume average of \mathbf{q} over the region $\mathcal{V} \setminus \nu_\alpha$ excluding medium α .

The local and macroscopic continuity equations for energy, momentum and particle number are summarised in Table 1. In colloidal suspensions, energy transport occurs primarily via heat conduction, which is much faster than particle transport. At a local and macroscopic scale, conservation of energy can therefore be described using the steady-state form of the heat equation, governed by the heat diffusion flux $\mathbf{j}_q = -\kappa \nabla T$, which couples to the gradient in temperature T via the thermal conductivity κ . At mechanical equilibrium,

Quantity	Local scale	Macroscopic scale
Energy	$\nabla \cdot \mathbf{j}_q = Q$	$\bar{\nabla} \cdot \langle \mathbf{j}_q \rangle = \langle Q \rangle$
Momentum	$\mathbf{f} + \nabla \cdot \boldsymbol{\sigma} = 0$	$\langle \mathbf{f} \rangle + \bar{\nabla} \cdot \langle \boldsymbol{\sigma} \rangle = 0$
Particle number	$\nabla \cdot \mathbf{J}_i = \Gamma_i$	$\partial_t \langle n_i \rangle + \bar{\nabla} \cdot \langle \mathbf{J}_i \rangle = \langle \Gamma_i \rangle$

Table 1: Local and macroscopic continuity equations for energy, momentum and particle number in a colloidal suspension. The fluxes \mathbf{j}_q , $\boldsymbol{\sigma}$ and \mathbf{J}_i correspond to the heat diffusion flux, stress tensor and particle flux of component i , respectively. \mathbf{f} is the body force density, whereas the source densities Q and Γ_i account for the production or consumption of heat and particles of component i , respectively. The term $\partial_t \langle n_i \rangle$ is the derivative of the volume-averaged component number density n_i with respect to time, describing the macroscopic evolution of component i .

the local and macroscopic momentum continuity equations are solved under the constraints of incompressible flow, expressed by

$$\nabla \cdot \mathbf{u} = 0, \quad (8)$$

$$\bar{\nabla} \cdot \langle \mathbf{u} \rangle = 0, \quad (9)$$

where \mathbf{u} is the local flow velocity and $\langle \mathbf{u} \rangle$ is the advective suspension velocity. The particle flux \mathbf{J}_i can also be expressed as $\mathbf{J}_i = n_i \mathbf{u} + \mathbf{j}_i$, where n_i is the component number density of component i . The local diffusion flux \mathbf{j}_i describes motion of the particles of component i relative to the flow velocity \mathbf{u} . If the index i refers to a component of a solid microphase ($i \in \nu_m$), where diffusion is prohibited, we simply have $\mathbf{j}_i = 0$. The local diffusion fluxes satisfy $\sum_i w_i \mathbf{j}_i = 0$, where the weighting factor w_i corresponds to the mass or volume of a particle of component i , respectively, depending on whether these fluxes describe motion relative to a local barycentric or volume-fixed frame. There is no need to specify whether \mathbf{u} corresponds to the barycentric or volume-averaged velocity of dV , provided that Eq. (8) is satisfied. The goal of homogenisation is to reduce the macroscopic continuity equations to linear differential equations in the macroscopic fields of temperature, flow velocity and component number densities. This nontrivial task is achieved by deriving linear constitutive relations for the macroscopic fluxes that are of the same form as the local ones, but instead describe the coupling to macroscopic gradients based on effective transport properties of the suspension. Indeed, analytical expressions of the effective thermal conductivity or dynamic viscosity of a suspension are usually obtained based on specific assumptions in the dilute limit, to first order in the microparticle volume fractions.[16, 17]

To describe colloidal diffusion, we introduce the decomposition $\mathbf{u} = \langle \mathbf{u} \rangle + \mathbf{u}'$, where \mathbf{u}' is the diffusion flow velocity, such that $\langle \mathbf{u}' \rangle = 0$ and $\nabla \cdot \mathbf{u}' = 0$. Hence, the local and macroscopic particle fluxes of component i can be written as $\mathbf{J}_i = n_i \langle \mathbf{u} \rangle + n_i \mathbf{u}' + \mathbf{j}_i$ and $\langle \mathbf{J}_i \rangle = \langle n_i \rangle \langle \mathbf{u} \rangle + \mathcal{J}_i$, where $\mathcal{J}_i = \langle n_i \mathbf{u}' \rangle + \langle \mathbf{j}_i \rangle$ is the macroscopic diffusion flux and $\langle n_i \mathbf{u}' \rangle$ is the macroscopic diffusion flow of component i . Since local diffusion is fast compared to diffusion flow inside the solution ($\mathbf{j}_i/n_i \gg \mathbf{u}'$ for $i \in \nu_n$), the local conservation of particle number for the solute and solvent components reduces to a steady-state equation given by $\nabla \cdot \mathbf{j}_i = \Gamma_i$ inside the advective frame of zero mean volume flux. To introduce the colloids as a macroscopic component of the suspension, we can consider any given microparticle species c , such that N_c identical colloids occupy a partial region ν_c of a homogeneous volume element \mathcal{V} . Note that the fluid surrounding these colloids may comprise other species of microparticles. The number of constituent component particles per colloid can be written as $\mathcal{N}_c = V \sum_j \langle n_j \rangle / N_c$, where the index j runs over all components that are part of the solid microphase

of the colloids. Assuming that the composition of a colloid remains largely unchanged by chemical reactions on its surface, the number density of the colloidal component can then be defined as $n_c = \sum_j \langle n_j \rangle / \mathcal{N}_c$, and the colloidal particle flux as $\mathbf{J}_c = \sum_j \langle \mathbf{J}_j \rangle / \mathcal{N}_c = n_c \langle \mathbf{u} \rangle + \mathcal{J}_c$. Introducing a corresponding chemical source density Γ_c , the colloidal continuity equation becomes

$$\frac{\partial n_c}{\partial t} + \langle \mathbf{u} \rangle \cdot \bar{\nabla} n_c + \bar{\nabla} \cdot \mathcal{J}_c = \Gamma_c. \quad (10)$$

Since components of the colloidal microphase cannot undergo local diffusion, the colloidal diffusion flux is a pure diffusion flow, given by $\mathcal{J}_c = n_c \langle \mathbf{u}' \rangle_{\nu_c}$, where $\langle \mathbf{u}' \rangle_{\nu_c} = \langle \mathbf{u} \rangle_{\nu_c} - \langle \mathbf{u} \rangle$ is the diffusion velocity of the colloids. Our aim is to close Eq. (10) by deriving a computable, continuum-statistical expression for the colloidal diffusion flux \mathcal{J}_c . To this end, we must distinguish the forces that drive flow from those that respond to flow under the constraint of incompressibility.

5 Thermodynamic forces and hydrodynamic stress in colloidal suspensions

We begin by decomposing the stress tensor $\boldsymbol{\sigma}$ into a hydrostatic stress $\boldsymbol{\sigma}_s$, and a hydrodynamic stress $\boldsymbol{\sigma}_d$ that vanishes in the absence of flow:

$$\boldsymbol{\sigma} = \boldsymbol{\sigma}_s + \boldsymbol{\sigma}_d, \quad (11)$$

where the letters "s" and "d" stand for "static" and "dynamic", respectively. The constitutive relation for the stress tensor takes the form $\boldsymbol{\sigma} = -P\mathbf{I} + \boldsymbol{\Sigma}$, where $P = \text{Tr } \boldsymbol{\sigma} / 3$ is the pressure, \mathbf{I} is the identity tensor, and $\boldsymbol{\Sigma}$ is the shear stress tensor. The pressure P couples to the solvent reservoir to enforce a mechanical equilibrium under incompressible flow. In suspensions, $\boldsymbol{\Sigma}$ consists of a purely viscous stress $\boldsymbol{\Sigma}_\eta$ inside the solution, and of a solid constraint stress $\boldsymbol{\Sigma}_m$ inside the microparticles. We can therefore write the shear stress tensor as a sum of two separate stress fields, such that $\boldsymbol{\Sigma} = \boldsymbol{\Sigma}_\eta + \boldsymbol{\Sigma}_m$. The linear constitutive relation for the viscous stress tensor under incompressible flow is given by $\boldsymbol{\Sigma}_\eta = \eta \mathbf{e}$, where η is the dynamic viscosity of the solution, and \mathbf{e} is the strain rate tensor, defined by $\mathbf{e} = (\nabla \mathbf{u} + \nabla^\dagger \mathbf{u}) / 2$. Since the microparticles are only in direct contact with the solution and hence under isotropic hydrostatic stress, we obtain the constitutive relations $\boldsymbol{\sigma}_s = -P_s \mathbf{I}$ and $\boldsymbol{\sigma}_d = -P_d \mathbf{I} + \boldsymbol{\Sigma}_m + \boldsymbol{\Sigma}_\eta$, such that $P = P_s + P_d$. Based on the Gibbs-Duhem equation, the hydrostatic pressure gradient can be written as $\nabla P_s = s \nabla T + \sum_i n_i \nabla \mu_i$, where s is the entropy density and μ_i is the chemical potential of component i . Whether mechanical equilibrium is enforced via a hydrostatic or hydrodynamic response of the solvent depends on the boundary conditions, noting that a hydrostatic equilibrium can only be maintained normal to a solid boundary that undergoes no net diffusion. The latter condition for hydrostatic equilibrium applies at the local scale, where it is a prerequisite for force-free colloidal motion, and at the macroscopic scale, where it enables a global hydrostatic equilibrium in a colloidal suspension confined within closed container walls.

For a clear distinction between thermodynamic forces and hydrodynamic stresses, the thermodynamic force density can now be introduced via

$$\mathcal{F} = \mathbf{f} - \nabla P_s. \quad (12)$$

To first order, the body force density is given by $\mathbf{f} = \sum_i n_i^{\text{eq}} (\mathbf{F}_i - \nabla \phi_i)$, where ϕ_i is the interfacial interaction potential of component i . The non-equilibrium body force \mathbf{F}_i acting on component i consists of an electric force and a gravitational force, such that $\mathbf{F}_i = e z_i \mathbf{E} + m_i \mathbf{g}$, where e is the elementary charge, z_i and m_i are the charge number and mass of a particle of component i , and \mathbf{E} and \mathbf{g} are the corresponding electric and gravitational field vectors. Overall electroneutrality of \mathcal{V} implies that $\langle \omega \rangle = 0$ and $\langle \mathcal{F} \rangle = \langle \rho \rangle \mathbf{g} - \langle \nabla P_s \rangle$,

where $\rho = \sum_i m_i n_i^{\text{eq}}$ is the mass density and $\omega = \sum_i e z_i n_i^{\text{eq}}$ is the electric charge density. The gravitational field vector \mathbf{g} is uniform throughout the suspension, whereas the non-equilibrium electric field \mathbf{E} satisfies $\epsilon^{\text{eq}} \nabla \cdot \mathbf{E} = 0$, where ϵ is the electric permittivity. At RTE, chemical equilibrium at the interfacial boundaries implies that the interfacial interaction potential ϕ_i of a component i can be absorbed into its chemical potential, such that $\hat{\mu}_i = \mu_i + \phi_i$, where $\hat{\mu}_i$ is the chemical potential of the non-equilibrium thermodynamic state of component i in the absence of interfacial interactions. To first order, the thermodynamic force density then takes non-equilibrium thermodynamic form[6]

$$\mathcal{F} = -\hat{h}^{\text{eq}} \frac{\nabla T}{T^{\text{eq}}} + \sum_i n_i^{\text{eq}} (\mathbf{F}_i - \nabla_T \hat{\mu}_i), \quad (13)$$

where ∇_T is the gradient at uniform temperature. The modified enthalpy density \hat{h} is given by $\hat{h} = h - \sum_i n_i H_i$, where h is the net enthalpy density and where $H_i = \hat{\mu}_i - T (\partial \hat{\mu}_i / \partial T)_{P_s, n_j}$ is the partial enthalpy per particle of component i . Inside regions where interfacial potential interactions and non-equilibrium body forces are absent, one simply has $\mathcal{F} = -\nabla P_s$. In view of Eq. (13), the thermodynamic force density is a linear combination of the form $\mathcal{F} = \sum_X \rho_X^{\text{eq}} \mathbf{X}$, due to the coupling of a thermodynamic force \mathbf{X} to a corresponding equilibrium scalar density ρ_X^{eq} . The thermodynamic forces are determined by the local continuity equations under slowly evolving boundary conditions and are uniform across \mathcal{V} if no interfacial boundaries are present. The disturbance of \mathcal{F} induced by the colloids relative to the bulk fluid can be expressed as $\delta \mathcal{F} = \sum_X (\delta \rho_X^{\text{eq}} \mathbf{X} + \rho_X^{\text{b|eq}} \delta \mathbf{X})$, where $\delta \rho_X^{\text{eq}}$ is the excess equilibrium density coupling to the local thermodynamic force \mathbf{X} . Notably, the expression of $\delta \mathcal{F}$ shows that such a disturbance can also be induced by a bulk equilibrium density $\rho_X^{\text{b|eq}}$ coupling to a thermodynamic force disturbance $\delta \mathbf{X}$ when the internal transport properties of the colloids differ from those of the fluid. Furthermore, the Curie symmetry principle implies that the local diffusion fluxes of an isotropic solution ($i \in \nu_\eta$) only couple to vectorial thermodynamic forces,[1] such that

$$\mathbf{j}_i = -L_{iq} \frac{\nabla T}{T^{\text{eq}}} + \sum_{j \in \nu_\eta} L_{ij} (\mathbf{F}_j - \nabla_T \hat{\mu}_j). \quad (14)$$

The Onsager transport coefficients L_{ij} and L_{iq} depend on the equilibrium number densities $\{n_j^{\text{eq}}\}$, but are independent of the thermodynamic forces. The diagonal Onsager coefficient can be written as $L_{ii} = n_i^{\text{eq}} / \xi_i$, where ξ_i is the friction coefficient of a particle of component i . At LTE, the cross-coupling coefficients in Eq. (14) satisfy the Onsager reciprocal relations $L_{kq} = L_{qk}$ and $L_{kj} = L_{jk}$, implying that they also describe the heat flux and diffusion flux of component j caused by a body force on component i , respectively.

With Eqs. (11) and (12), the local and macroscopic momentum continuity equations become

$$\mathcal{F} + \nabla \cdot \boldsymbol{\sigma}_d = 0, \quad (15)$$

$$\langle \rho \rangle \mathbf{g} - \langle \nabla P_s \rangle + \langle \nabla \cdot \boldsymbol{\sigma}_d \rangle = 0. \quad (16)$$

At least one of the solvent components must be able to generate a hydrostatic pressure gradient ∇p that balances precisely those hydrostatic forces that do not drive flow. A representative example is given by a chemically active colloid with a spherically symmetric chemical source density of solute on its surface, which leads to no net motion.[15] The effective force density that drives flow is therefore given by $\mathcal{F} - \nabla p$. Note that $p = 0$ inside the microparticles and that p may not coincide with the net hydrostatic solvent pressure, since an electrically polarisable solvent can also drive flow when subjected to an electric field.[1] Furthermore, the local and macroscopic hydrodynamic stress tensors of a homogeneous suspension have the same constitutive

forms,[15] such that $\langle \nabla \cdot \boldsymbol{\sigma}_d \rangle = \bar{\nabla} \cdot \langle \boldsymbol{\sigma}_d \rangle = \bar{\nabla} \cdot (-\bar{P}_d \mathbf{I} + \bar{\eta} \langle \mathbf{e} \rangle)$, where \bar{P}_d and $\bar{\eta}$ are the hydrodynamic pressure and dynamic viscosity of the suspension, respectively, and where $\langle \mathbf{e} \rangle = (\bar{\nabla} \langle \mathbf{u} \rangle + \bar{\nabla}^T \langle \mathbf{u} \rangle) / 2$ is the strain rate tensor of the advective velocity $\langle \mathbf{u} \rangle$. The advective velocity can then be determined from Eq. (16), which also describes the advection of a bulk solution in the dilute limit. If boundary conditions allow for advection, Eq. (16) reduces to

$$\langle \rho \rangle \mathbf{g} - \bar{\nabla} \bar{\Pi} + \bar{\nabla} \cdot \langle \boldsymbol{\sigma}_d \rangle = 0, \quad (17)$$

where we have introduced the osmotic pressure $\bar{\Pi}$ of the suspension via $\bar{\nabla} \bar{\Pi} = \langle \nabla (P_s - p) \rangle$. If the suspension is at hydrostatic equilibrium, then the hydrostatic response of the solvent is instead fixed by

$$\langle \nabla p \rangle = \langle \rho \rangle \mathbf{g} - \bar{\nabla} \bar{\Pi}. \quad (18)$$

In this context, it is instructive to consider two suspensions at hydrostatic equilibrium, contained in two identical vessels kept at the same hydrostatic pressure at the top. At a given height z_0 , the vessels are connected by a narrow horizontal channel of length L (aligned along x). In particular, the boundary conditions at the channel ends only allow solvent to pass into or out of the channel, which remains void of solutes or microparticles. We assume no interfacial potential interaction between the solvent and the channel walls and consider an osmotic pressure difference between the vessels due to a difference in solute or microparticle number density. Since $\langle \partial P_s / \partial x \rangle = 0$, a hydrostatic solvent pressure gradient $\langle \partial p / \partial x \rangle = -\Delta \bar{\Pi} / L$ is established along the channel, where $\Delta \bar{\Pi} = \bar{\Pi}_{x=L} - \bar{\Pi}_{x=0}$ is the corresponding osmotic pressure difference. Projection of Eq. (16) onto x then yields $-\langle \partial p / \partial x \rangle + \langle \nabla \cdot \boldsymbol{\sigma}_d \rangle = 0$, showing that the gradient of the hydrostatic pressure p now acts as a driving force of flow inside the channel. To preserve the notion of $\langle \partial p / \partial x \rangle$ as a hydrostatic response, the pressure gradient across the channel can instead be interpreted as an osmotic disturbance of $-\Delta \bar{\Pi} / L$ relative to the bulk hydrostatic pressure gradient $\langle \partial P_s / \partial x \rangle = 0$ across the two vessels. We can hence write

$$\Delta \bar{\Pi} + L \bar{\nabla} \cdot \langle \boldsymbol{\sigma}_d \rangle = 0. \quad (19)$$

This momentum balance equation describes the effect of classical osmosis through a semi-permeable membrane, driving solvent flow into the vessel at higher osmotic pressure. Similarly, phoretic colloidal motion occurs when interfacial boundaries induce local force disturbances relative to the bulk fluid. A crucial insight gained from the case of classical osmosis is that such disturbances can arise solely from boundary conditions when interfacial potential interactions are absent. In contrast to a fixed semi-permeable membrane, however, a colloid is a freely moving object whose interactions with the fluid cannot inject momentum into the system. As a result, the combined motion of the colloid and the induced fluid flow must be an overall force-free motion relative to the advective frame of the suspension.

6 Reciprocal formulation of colloidal diffusion

To close the colloidal continuity equation, we require an expression for the colloidal diffusion flux. Hence, our aim is to derive a computable, continuum-statistical form of the volume-averaged velocity $\mathbf{v}_c = \langle \mathbf{u} \rangle_{\nu_c}$ of an ensemble of $N_c = n_c V$ colloids relative to the advective velocity $\langle \mathbf{u} \rangle$. For a homogeneous suspension, we now show that this can be achieved via application of the LRT by exploiting the auxiliary flow problem of colloidal sedimentation, together with the statistical invariance of hydrodynamic stress disturbances under translation.

In the auxiliary flow problem of colloidal sedimentation ("*"), a uniform body force \mathbf{F}^* is applied to every colloid, corresponding to a momentum continuity equation $\mathbf{f}^* + \nabla \cdot \boldsymbol{\sigma}_d^* = 0$, where \mathbf{f}^* takes the value $N_c \mathbf{F}^* / V_c$ inside the colloids and zero elsewhere. The flow induced by sedimentation is a diffusion flow, such

that $\langle \mathbf{u}^* \rangle = 0$. Each colloid sediments at a given velocity that may vary across the ensemble. The force \mathbf{F}^* is therefore chosen so that the mean sedimentation velocity equals the colloidal velocity \mathbf{v}_c , such that

$$\langle \mathbf{u}^* \rangle_{\mathbf{v}_c} = \mathbf{v}_c. \quad (20)$$

Under kinematic reversibility, the corresponding flow velocity and hydrodynamic stress of a homogeneous suspension are described by tensorial relations that are linear in \mathbf{v}_c . [14, 18] We can therefore write

$$\mathbf{u}^* = \mathbf{U}_c^* \cdot \mathbf{v}_c, \quad (21)$$

$$\boldsymbol{\sigma}_d^* = \mathcal{P}_c^* \cdot \mathbf{v}_c, \quad (22)$$

where \mathbf{U}_c^* and \mathcal{P}_c^* are the symmetric Stokes flow tensor and Stokes stress tensor, respectively. The Stokes flow tensor \mathbf{U}_c^* satisfies

$$\nabla \cdot \mathbf{U}_c^* = 0, \quad (23)$$

$$\langle \mathbf{U}_c^* \rangle = 0, \quad (24)$$

$$\langle \mathbf{U}_c^* \rangle_{\mathbf{v}_c} = \mathbf{I}. \quad (25)$$

In addition, we have $\mathbf{F}^* = \boldsymbol{\xi}_c \cdot \mathbf{v}_c$, where the Stokes friction tensor $\boldsymbol{\xi}_c$ of the colloids is related to the hydrodynamic traction tensor $\mathbf{T}_c^* = \mathcal{P}_c^* \cdot \mathbf{n}$ via $N_c \boldsymbol{\xi}_c = -\oint_{\partial \nu_c} \mathbf{T}_c^* dS$, where \mathbf{n} is the unit normal vector pointing out of the corresponding boundaries.

To derive the LRT for a representative volume element of a colloidal suspension, we first follow the standard procedure of contracting the forces from the local momentum continuity equation of each problem with the flow velocity of the other problem. [18, 19] However, rather than using the Cauchy form of the momentum continuity equation, as given in Table 1, we use its form in terms of the thermodynamic force density and hydrodynamic stress, given by Eq. (15). Since both contractions are zero, equating them gives

$$\mathbf{u} \cdot (\mathbf{f}^* + \nabla \cdot \boldsymbol{\sigma}_d^*) = \mathbf{u}^* \cdot (\mathcal{F} + \nabla \cdot \boldsymbol{\sigma}_d). \quad (26)$$

Collecting the terms related to the hydrodynamic stresses $\boldsymbol{\sigma}_d$ and $\boldsymbol{\sigma}_d^*$ on the right-hand side, we obtain

$$\mathbf{u}^* \cdot \mathcal{F} - \mathbf{u} \cdot \mathbf{f}^* = \mathbf{u} \cdot (\nabla \cdot \boldsymbol{\sigma}_d^*) - \mathbf{u}^* \cdot (\nabla \cdot \boldsymbol{\sigma}_d). \quad (27)$$

Each term on the right-hand side can further be rewritten using the identity $\mathbf{u} \cdot (\nabla \cdot \boldsymbol{\sigma}) = \nabla \cdot (\mathbf{u} \cdot \boldsymbol{\sigma}) - \boldsymbol{\sigma} : \nabla \mathbf{u}$, yielding $\mathbf{u}^* \cdot \mathcal{F} - \mathbf{u} \cdot \mathbf{f}^* = \nabla \cdot (\mathbf{u} \cdot \boldsymbol{\sigma}_d^* - \mathbf{u}^* \cdot \boldsymbol{\sigma}_d) + \boldsymbol{\sigma}_d : \nabla \mathbf{u}^* - \boldsymbol{\sigma}_d^* : \nabla \mathbf{u}$. The LRT relies on the symmetry of the last two terms in this relation. Using Eq. (8) and the constitutive form of the hydrodynamic stress in both flow problems, we have $\boldsymbol{\sigma}_d : \nabla \mathbf{u}^* = \boldsymbol{\Sigma}_m : \nabla \mathbf{u}^* + 2\eta \mathbf{e} : \mathbf{e}^*$. As the dynamic viscosity η is the same in both flow problems under kinematic reversibility, the last term on the right-hand side is symmetric in the interchange of \mathbf{e} and \mathbf{e}^* . We can therefore write $\boldsymbol{\sigma}_d : \nabla \mathbf{u}^* - \boldsymbol{\sigma}_d^* : \nabla \mathbf{u} = \boldsymbol{\Sigma}_m : \nabla \mathbf{u}^* - \boldsymbol{\Sigma}_m^* : \nabla \mathbf{u}$. However, the terms on the right-hand side only refer to regions of \mathcal{V} occupied by the microparticles, inside which flow velocity gradients are forbidden. Hence, $\boldsymbol{\sigma}_d : \nabla \mathbf{u}^* - \boldsymbol{\sigma}_d^* : \nabla \mathbf{u} = 0$, and Eq. (27) reduces to

$$\mathbf{u}^* \cdot \mathcal{F} - \mathbf{u} \cdot \mathbf{f}^* = \nabla \cdot (\mathbf{u} \cdot \boldsymbol{\sigma}_d^* - \mathbf{u}^* \cdot \boldsymbol{\sigma}_d). \quad (28)$$

Eq. (28) is independent of the flow velocity gradient $\nabla \mathbf{u}$ and can therefore be interpreted as a continuum-mechanical manifestation of the Curie symmetry principle.

In contrast to previous treatments, [18, 10, 12, 13] where Eq. (28) is integrated over the partial volume of the fluid only, we integrate it over the entire representative volume element \mathcal{V} , giving

$$\underbrace{\int_{\mathcal{V}} \mathbf{u}^* \cdot \mathcal{F} d^3 \mathbf{r}}_{I_1} - \underbrace{\int_{\mathcal{V}} \mathbf{u} \cdot \mathbf{f}^* d^3 \mathbf{r}}_{I_2} = \underbrace{\int_{\mathcal{V}} \nabla \cdot (\mathbf{u} \cdot \boldsymbol{\sigma}_d^* - \mathbf{u}^* \cdot \boldsymbol{\sigma}_d) d^3 \mathbf{r}}_{I_3}. \quad (29)$$

Based on the relations for the auxiliary flow problem, integrals I_1 and I_2 can be re-expressed as

$$I_1 = \mathbf{v}_c \cdot \int_{\mathcal{V}} \mathbf{U}_c^* \cdot \mathcal{F} d^3\mathbf{r}, \quad (30)$$

$$I_2 = N_c \mathbf{v}_c \cdot \boldsymbol{\xi}_c \cdot \mathbf{v}_c. \quad (31)$$

Applying Gauss' theorem to integral I_3 yields

$$I_3 = \oint_{\partial\mathcal{V}} (\mathbf{u} \cdot \boldsymbol{\sigma}_d^* - \mathbf{u}^* \cdot \boldsymbol{\sigma}_d) \cdot \mathbf{n} dS - \oint_{\partial\nu_m} (\mathbf{u}^{\parallel} \cdot \boldsymbol{\sigma}_d^* - \mathbf{u}^{\parallel*} \cdot \boldsymbol{\sigma}_d) \cdot \mathbf{n} dS, \quad (32)$$

where \mathbf{u}^{\parallel} and $\mathbf{u}^{\parallel*}$ are tangential slip velocities at the surfaces $\partial\nu_m$ of the microparticles in each flow problem. As thermal transpiration is negligible at low Knudsen number,[20] these slip velocities satisfy the Navier slip boundary condition:[21]

$$\mathbf{u}^{\parallel} = \mathbf{u}_a + \frac{l_{\text{slip}}}{\eta} (\mathbf{I} - \mathbf{nn}) \cdot (\mathbf{n} \cdot \boldsymbol{\sigma}_d), \quad (33)$$

$$\mathbf{u}^{\parallel*} = \frac{l_{\text{slip}}}{\eta} (\mathbf{I} - \mathbf{nn}) \cdot (\mathbf{n} \cdot \boldsymbol{\sigma}_d^*). \quad (34)$$

In the actual flow problem, the active slip velocity profile \mathbf{u}_a is defined on all microparticle surfaces. In our treatment, this active slip velocity represents a boundary-layer treatment of force-free self-propulsion mechanisms stemming from non-hydrostatic forces that are not described by the thermodynamic force density \mathcal{F} , like those due to ciliary motion.[22, 23] As for dynamic viscosity, the principle of kinematic reversibility justifies the use of the same hydrodynamic slip length l_{slip} in both flow problems. Let us consider the integral of the term $\mathbf{u}^{\parallel} \cdot \boldsymbol{\sigma}_d^* \cdot \mathbf{n}$ over the interfaces in Eq. (32). Substituting Eq. (33), we can write $((\mathbf{I} - \mathbf{nn}) \cdot (\mathbf{n} \cdot \boldsymbol{\sigma}_d) \cdot \boldsymbol{\sigma}_d^*) \cdot \mathbf{n} = (\mathbf{n} \cdot \boldsymbol{\sigma}_d) \cdot (\mathbf{n} \cdot \boldsymbol{\sigma}_d^*) - (\mathbf{n} \cdot \boldsymbol{\sigma}_d \cdot \mathbf{n}) \cdot (\mathbf{n} \cdot \boldsymbol{\sigma}_d^* \cdot \mathbf{n})$, which is symmetric in the interchange of $\boldsymbol{\sigma}_d$ and $\boldsymbol{\sigma}_d^*$. Hence, we obtain

$$\oint_{\partial\nu_m} (\mathbf{u}^{\parallel} \cdot \boldsymbol{\sigma}_d^* - \mathbf{u}^{\parallel*} \cdot \boldsymbol{\sigma}_d) \cdot \mathbf{n} dS = \mathbf{v}_c \cdot \oint_{\partial\nu_m} \mathbf{T}_c^* \cdot \mathbf{u}_a dS. \quad (35)$$

To describe colloidal diffusion, we introduce the decompositions $\mathbf{u} = \mathbf{u}' + \langle \mathbf{u} \rangle$ and $\boldsymbol{\sigma}_d = \boldsymbol{\sigma}'_d + \langle \boldsymbol{\sigma}_d \rangle$ into the surface integral over $\partial\mathcal{V}$, giving

$$\oint_{\partial\mathcal{V}} (\mathbf{u} \cdot \boldsymbol{\sigma}_d^* - \mathbf{u}^* \cdot \boldsymbol{\sigma}_d) \cdot \mathbf{n} dS = -\mathbf{v}_c \cdot N_c \boldsymbol{\xi}_c \cdot \langle \mathbf{u} \rangle + \oint_{\partial\mathcal{V}} (\mathbf{u}' \cdot \boldsymbol{\sigma}_d^* - \mathbf{u}^* \cdot \boldsymbol{\sigma}'_d) \cdot \mathbf{n} dS. \quad (36)$$

In the dilute limit, the flow velocities \mathbf{u}' and \mathbf{u}^* and hydrodynamic stress tensors $\boldsymbol{\sigma}'_d$ and $\boldsymbol{\sigma}_d^*$ are known to decay as $1/r$ and $1/r^2$ inside the solution, respectively,[18, 24] implying that the surface integrals over $\partial\mathcal{V}$ in Eq. (36) vanish. For a homogeneous suspension, the vanishing of these surface integrals is instead justified by the statistical invariance of these fields under translation. We therefore have

$$\oint_{\partial\mathcal{V}} (\mathbf{u}' \cdot \boldsymbol{\sigma}_d^* - \mathbf{u}^* \cdot \boldsymbol{\sigma}'_d) \cdot \mathbf{n} dS = 0. \quad (37)$$

Notably, Eqs. (35) and (37) rely on the specific properties of hydrodynamic stress induced by diffusion flow, highlighting the necessity of decoupling this stress from the hydrostatic stress. Integral I_3 thus reduces to

$$I_3 = -\mathbf{v}_c \cdot N_c \boldsymbol{\xi}_c \cdot \langle \mathbf{u} \rangle - \mathbf{v}_c \cdot \oint_{\partial\nu_m} \mathbf{T}_c^* \cdot \mathbf{u}_a dS. \quad (38)$$

Using Eqs. (30), (31) and (38) in Eq. (29), the colloidal velocity relative to advection, or colloidal diffusion velocity, can be identified as

$$\mathbf{v}_c - \langle \mathbf{u} \rangle = \frac{1}{N_c \boldsymbol{\xi}_c} \cdot \left(\int_{\mathcal{V}} \mathbf{U}_c^* \cdot \mathcal{F} d^3 \mathbf{r} + \oint_{\partial \nu_m} \mathbf{T}_c^* \cdot \mathbf{u}_a dS \right), \quad (39)$$

where we note that the corresponding colloidal diffusion flux is simply given by $\mathcal{J}_c = n_c (\mathbf{v}_c - \langle \mathbf{u} \rangle)$. Crucially, the colloidal diffusion velocity $\mathbf{v}_c - \langle \mathbf{u} \rangle$ only refers to the hydrodynamic tensors \mathbf{U}_c^* and \mathbf{T}_c^* of the auxiliary Stokes problem of colloidal sedimentation, which is well established and feasible to study numerically by applying a flow to an ensemble of stationary colloids. In the fluid region, these tensors account for the hydrodynamic drag on the colloids due to forces on the fluid components, which vanishes in the Hückel limit where the colloid's hydrodynamic radius tends to zero.[25] The first term in Eq. (39) describes diffusion due to vectorial thermodynamic forces, including sedimentation and phoretic transport in response to externally applied or self-generated thermodynamic forces. The latter forces are caused by chemical or thermal activity, whereas the forces giving rise to the second term in Eq. (39) stem from ciliary activity. In this context, it should be noted that any form of activity eventually produces correlations in colloidal motion that result in a breakdown of homogeneity and isotropy inside the suspension.[26]

To demonstrate the connection to Onsager's reciprocal theory, we now substitute Eq. (13) into Eq. (39), yielding

$$\mathcal{J}_c = -\frac{1}{\boldsymbol{\xi}_c} \cdot \left\langle \hat{h}^{\text{eq}} \mathbf{U}_c^* \cdot \frac{\nabla T}{T^{\text{eq}}} \right\rangle + \frac{1}{\boldsymbol{\xi}_c} \cdot \sum_i \langle n_i^{\text{eq}} \mathbf{U}_c^* \cdot (\mathbf{F}_i - \nabla_T \dot{\mu}_i) \rangle + \frac{1}{\boldsymbol{\xi}_c} \cdot \oint_{\partial \nu_m} \mathbf{T}_c^* \cdot \mathbf{u}_a dS. \quad (40)$$

Indeed, the quantities $h^{\text{eq}} \mathbf{U}_c^*$ and $n_i^{\text{eq}} \mathbf{U}_c^*$ can be identified as the local flows of heat and component particles induced by colloidal sedimentation, respectively. If the thermodynamic forces are assumed uniform over \mathcal{V} , which amounts to ignoring interfacial boundary conditions inside \mathcal{V} , we obtain

$$\mathcal{J}_c = -\mathbf{L}_{cq} \cdot \frac{\nabla T}{T^{\text{eq}}} + \sum_i \mathbf{L}_{ci} \cdot (\mathbf{F}_i - \nabla_T \dot{\mu}_i) + \frac{1}{\boldsymbol{\xi}_c} \cdot \oint_{\partial \nu_m} \mathbf{T}_c^* \cdot \mathbf{u}_a dS, \quad (41)$$

with $\mathbf{L}_{cq} = \boldsymbol{\xi}_c^{-1} \cdot \langle \hat{h}^{\text{eq}} \mathbf{U}_c^* \rangle$ and $\mathbf{L}_{ci} = \boldsymbol{\xi}_c^{-1} \cdot \langle n_i^{\text{eq}} \mathbf{U}_c^* \rangle$. Since transport tensors reduce to scalars in a homogeneous, isotropic suspension, such that $\mathbf{L}_{cq} = L_{cq} \mathbf{I}$, $\mathbf{L}_{ci} = L_{ci} \mathbf{I}$ and $\boldsymbol{\xi}_c = \xi_c \mathbf{I}$, we finally recover the standard scalar form of the Onsager reciprocal relations for colloidal diffusion:

$$L_{cq} = L_{qc} = \frac{1}{\xi_c} \langle \hat{h}^{\text{eq}} \mathbf{U}_c^* \rangle, \quad (42)$$

$$L_{ci} = L_{ic} = \frac{1}{\xi_c} \langle n_i^{\text{eq}} \mathbf{U}_c^* \rangle. \quad (43)$$

The Hückel limit, for which $\mathbf{U}_c^* = 0$ in the fluid region, thus corresponds to the case of vanishing hydrodynamic cross-coupling between the colloidal diffusion flux and the thermodynamic forces in the fluid. Based on the assumption of uniform gradients, we also conclude that the standard scalar form of the Onsager reciprocal relations cannot account for active motion.

To obtain analytical expressions for the auxiliary hydrodynamic tensors, we may consider the dilute limit where the diffusion of a single colloid can be studied inside an unbounded solution. Assuming uniform viscosity ($\eta = \eta^b$), the friction tensor of a spherical, homogeneous colloid of hydrodynamic radius R is given by

$$\boldsymbol{\xi}_c = \xi_c \mathbf{I} = 6\pi s \eta R \mathbf{I}, \quad (44)$$

where the hydrodynamic slip parameter $s = (1 + 2l_{\text{slip}}/R)/(1 + 3l_{\text{slip}}/R)$ takes the value 1 for a no-slip boundary condition and 2/3 for a perfect-slip boundary condition. To leading order, the backflow required to satisfy Eq. (24) decays with $1/L$, where L is the macroscopic length scale. In an unbounded solution, the auxiliary hydrodynamic tensors therefore take the familiar forms:

$$\mathbf{U}_c^* = \frac{3R}{4r} \left[s(\mathbf{I} + \hat{\mathbf{r}}\hat{\mathbf{r}}) - \left(s - \frac{2}{3} \right) \frac{R^2}{r^2} (3\hat{\mathbf{r}}\hat{\mathbf{r}} - \mathbf{I}) \right], \quad (45)$$

$$\mathbf{T}_c^* = -\frac{9\eta R}{2r^2} \left[s\hat{\mathbf{r}}\hat{\mathbf{r}} - \left(s - \frac{2}{3} \right) \frac{R^2}{r^2} (3\hat{\mathbf{r}}\hat{\mathbf{r}} - \mathbf{I}) \right], \quad (46)$$

where r is the radial distance from the hydrodynamic centre of the colloid and $\hat{\mathbf{r}}$ is the outward-pointing radial unit vector. Alternatively, Eq. (46) can also be expressed as $\mathbf{T}_c^* = 9\eta s R \mathbf{I} / (2r^2) - 6\eta \mathbf{U}_c^* / r$. With Eqs. (44) and (46), the contribution due to ciliary motion in Eq. (39) then reduces to the colloidal swimming velocity $\mathbf{v}_{\text{swim}} = \boldsymbol{\xi}_c^{-1} \cdot \oint_{\partial\nu_c} (\mathbf{T}_c^* \cdot \mathbf{u}_a) dS$, which becomes

$$\mathbf{v}_{\text{swim}} = -\left(3 - \frac{2}{s} \right) \frac{1}{4\pi R^2} \oint_{\partial\nu_c} \mathbf{u}_a dS = -\frac{\langle \mathbf{u}_a \rangle_{\partial\nu_c}}{1 + 2l_{\text{slip}}}. \quad (47)$$

This expression vanishes for a perfect-slip boundary condition ($s = 2/3$), whereas it reduces to the familiar form $-(4\pi R^2)^{-1} \oint_{\partial\nu_c} \mathbf{u}_a dS$ for a no-slip boundary condition ($s = 1$), [27] thereby generalising the latter result to arbitrary hydrodynamic slippage at the colloidal surface. A vanishing swimming velocity for $s = 2/3$ is indeed expected, since a perfectly slipping ciliary envelope cannot exert a tangential force on the fluid.

7 Continuum-statistical formulation of colloidal diffusion

To obtain a computable continuum-statistical form of the colloidal diffusion flux, we must eliminate from Eq. (39) the thermodynamic forces arising within the solid microphase of the colloids, where the equation of state usually remains unknown. To this end, we consider the volume integral of \mathcal{F} over \mathcal{V} and write it as a sum of integrals over the colloidal region ν_c and fluid region $\tilde{\nu}$, which yields $\int_{\nu_c} \mathcal{F} d^3\mathbf{r} + \int_{\tilde{\nu}} \mathcal{F} d^3\mathbf{r} = \int_{\mathcal{V}} \rho d^3\mathbf{r} \mathbf{g} - \int_{\mathcal{V}} \nabla P_s d^3\mathbf{r}$ due to electroneutrality of \mathcal{V} . Based on Eq. (25), the volume integral in Eq. (39) can be written as $\int_{\mathcal{V}} \mathbf{U}_c^* \cdot \mathcal{F} d^3\mathbf{r} = \int_{\nu_c} \mathcal{F} d^3\mathbf{r} + \int_{\tilde{\nu}} \mathbf{U}_c^* \cdot \mathcal{F} d^3\mathbf{r}$. Combining these two relations gives

$$\int_{\mathcal{V}} \mathbf{U}_c^* \cdot \mathcal{F} d^3\mathbf{r} = \int_{\tilde{\nu}} (\mathbf{U}_c^* - \mathbf{I}) \cdot \mathcal{F} d^3\mathbf{r} + \int_{\mathcal{V}} \rho d^3\mathbf{r} \mathbf{g} - \int_{\mathcal{V}} \nabla P_s d^3\mathbf{r}. \quad (48)$$

In the fluid region, the thermodynamic force density $\mathcal{F} = \delta\mathcal{F} + \mathcal{F}^b$ can be decomposed into a bulk contribution \mathcal{F}^b and a disturbance $\delta\mathcal{F}$ induced by the colloids relative to the bulk fluid. Although the bulk fluid may not be electroneutral everywhere within \mathcal{V} if it contains other species of microparticles ($\omega^b \neq 0$), it must remain overall electroneutral over \mathcal{V} , such that $\int_{\mathcal{V}} \mathcal{F}^b d^3\mathbf{r} = \int_{\tilde{\nu}} \rho^b d^3\mathbf{r} \mathbf{g} - \int_{\mathcal{V}} \nabla P_s^b d^3\mathbf{r}$, where P_s^b is the hydrostatic pressure of the bulk fluid. Noting that the thermodynamic force density \mathcal{F}^b of a homogeneous bulk fluid has no statistical correlation with the Stokes flow tensor \mathbf{U}_c^* , we have $\int_{\tilde{\nu}} (\mathbf{U}_c^* - \mathbf{I}) \cdot \mathcal{F} d^3\mathbf{r} = \int_{\tilde{\nu}} (\mathbf{U}_c^* - \mathbf{I}) \cdot \delta\mathcal{F} d^3\mathbf{r} - \int_{\mathcal{V}} \mathcal{F}^b d^3\mathbf{r}$, where we also used Eqs. (24) and (25).

The induced hydrostatic response δp of the solvent cannot drive colloidal diffusion, implying that $\oint_{\partial\nu_c} \delta p \mathbf{n} dS = 0$. As a result, δp must follow a spherically symmetric decay far away from a colloid in the dilute limit and fulfill a statistical invariance under translation in a homogeneous suspension, yielding $\int_{\tilde{\nu}} \nabla \delta p d^3\mathbf{r} = \oint_{\partial\nu} \delta p \mathbf{n} dS - \oint_{\partial\nu_c} \delta p \mathbf{n} dS = 0$. Based on Eq. (23), we further have $\mathbf{U}_c^* \cdot \nabla \delta p = \nabla \cdot (\delta p \mathbf{U}_c^*)$, from which it

follows with $\mathbf{U}_c^* \cdot \mathbf{n} = \mathbf{I}$ on $\partial\nu_c$ that $\int_{\bar{\nu}} \mathbf{U}_c^* \cdot \nabla \delta p d^3 \mathbf{r} = \oint_{\partial\mathcal{V}} \delta p \mathbf{U}_c^* \cdot \mathbf{n} dS - \oint_{\partial\nu_c} \delta p \mathbf{U}_c^* \cdot \mathbf{n} dS = 0$. Hence, we obtain

$$\int_{\bar{\nu}} (\mathbf{U}_c^* - \mathbf{I}) \cdot \nabla \delta p d^3 \mathbf{r} = 0, \quad (49)$$

showing that precisely those hydrostatic forces that do not drive colloidal diffusion vanish under the form $\int_{\bar{\nu}} (\mathbf{U}_c^* - \mathbf{I}) \cdot [\dots] d^3 \mathbf{r}$, as expected. As illustrated in Fig. 3, the colloidal osmotic pressure $\bar{\Pi}_c$ can be introduced via

$$\bar{\nabla} \bar{\Pi}_c = \langle \nabla (P_s - P_s^b) \rangle. \quad (50)$$

A crucial consequence of the condition of RTE is that the colloidal osmotic pressure derives from a thermodynamic equation of state.[28] Eq. (50) can be understood as a generalisation of the well-known force-free condition, which is usually formulated in the dilute limit. If the hydrostatic pressure is uniform in the bulk fluid, Eq. (50) becomes $\int_{\mathcal{V}} \nabla P_s d^3 \mathbf{r} = 0$ for a single colloid inside \mathcal{V} when thermal fluctuations are neglected. In the absence of gravity, the macroscopic momentum balance equation given by Eq. (16) then indeed reduces to $\langle \nabla \cdot \boldsymbol{\sigma}_d \rangle = 0$, which corresponds to the force-free condition.[7] Using Eqs. (48)-(50) in Eq. (39), the colloidal diffusion velocity finally takes the continuum-statistical form

$$\begin{aligned} \mathbf{v}_c - \langle \mathbf{u} \rangle = \frac{1}{N_c \xi_c} \cdot & \left[\int_{\bar{\nu}} (\mathbf{U}_c^* - \mathbf{I}) \cdot \mathcal{F}_{\text{ph}} d^3 \mathbf{r} \right. \\ & + \left(\int_{\nu_c} \delta \rho d^3 \mathbf{r} + \int_{\bar{\nu}} \delta \rho \mathbf{U}_c^* d^3 \mathbf{r} \right) \cdot \mathbf{g} \\ & \left. - V \bar{\nabla} \bar{\Pi}_c + \oint_{\partial\nu_m} \mathbf{T}_c^* \cdot \mathbf{u}_a dS \right], \end{aligned} \quad (51)$$

where $\mathbf{U}_c^* - \mathbf{I}$ represents the fluid flow velocity induced by sedimentation in the rest frame of the colloids. The phoretic force density \mathcal{F}_{ph} is given by

$$\mathcal{F}_{\text{ph}} = \delta \left[\omega \mathbf{E} - \hbar^{\text{eq}} \frac{\nabla T}{T^{\text{eq}}} - \left(\sum_i n_i^{\text{eq}} \nabla_T \hat{\mu}_i - \nabla p \right) \right]. \quad (52)$$

In view of Eq. (49), the term ∇p in Eq. (52) is merely a bookkeeping term, showing that those hydrostatic forces that cannot drive flow are balanced by the hydrostatic response of the solvent. Inside regions where interfacial potential interactions and electric fields are absent, Eq. (52) reduces to

$$\mathcal{F}_{\text{ph}} = -\nabla \delta (P_s - p) = -\nabla \delta \Pi, \quad (53)$$

where the local osmotic pressure $\Pi = P_s - p$ corresponds to the hydrostatic pressure relative to the response of the solvent.

To first order in the non-equilibrium forces, Eq. (51) provides a complete description of colloidal diffusion in a homogeneous suspension and reduces to the diffusion velocity of a single colloid in the dilute limit. Within our continuum-statistical formulation, only the fourth term due to ciliary activity retains its original form. The first term represents (self-)phoretic motion, which is consistent with its force-free nature: overall, fluid flows in the direction of the phoretic force density \mathcal{F}_{ph} , whereas the colloid is pushed in the opposite direction. In the dilute limit, the BLA for phoretic motion of a single colloid, applied to thermophoresis by Derjaguin[4] and known as the Smoluchowski limit in electrophoresis, can be recovered from this term by assuming uniform gradients and a no-slip hydrodynamic boundary condition. Using Eq. (45) and expanding this term to first order in $z = r - R \ll R$, one then recovers the well-known BLA expression $\int_{\bar{\nu}} (\mathbf{U}_c^* - \mathbf{I}) \mathcal{F}_{\text{ph}} d^3 \mathbf{r} \approx$

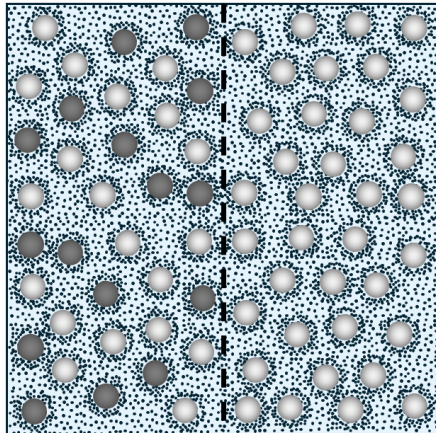


Figure 3: From a continuum-mechanical perspective, the osmotic pressure of the colloids (dark spheres) is defined as the pressure difference across a semi-permeable membrane (dashed line) separating the bulk fluid from the suspension.

$-4\pi R^2 \int_0^\infty z \mathcal{F}_{\text{ph}} dz$. [6] The second term in Eq. (51) represents buoyant sedimentation, accounting for the buoyant mass $\int_{V_c} \delta\rho d^3\mathbf{r}$ of the colloids and for the hydrodynamic drag caused by the fluid excess weight via $\int_V \delta\rho \mathbf{U}_c^* d^3\mathbf{r}$. The third term has a purely continuum-statistical nature, accounting for the average colloidal motion due to thermal fluctuations and hydrostatic many-body interactions via the colloidal osmotic pressure gradient $\nabla \bar{\Pi}_c$. [28] Notably, all terms in Eq. (51) follow from a single application of the LRT using the auxiliary Stokes flow problem of colloidal sedimentation.

Eq. (51) also aligns with a previously developed treatment based on Onsager reciprocity. [6] The agreement becomes apparent by noting that the definition of the phoretic force density used here includes the thermodynamic force disturbances relative to the bulk fluid, which were considered separately in our previous treatment. The resulting predictions have been verified numerically using mesoscale-molecular simulations, [29] successfully applied to experimental data on thermophoresis of DNA, [30] and used to generalise the Henry function for electrophoresis and the Ruckenstein function for thermophoresis to arbitrary hydrodynamic slippage and interfacial excess layer thicknesses. [31] However, our previous approach simply postulated continuum-mechanical reciprocal relations, did not account for ciliary motion, and evaluated the contributions to the colloidal velocity per thermodynamic force inside a suspension at hydrostatic equilibrium, without clarifying the role of the solvent in momentum relaxation. The continuum-statistical framework presented here overcomes these limitations, demonstrating that reciprocity in colloidal motion emerges from kinematic reversibility at the continuum scale, encompassing the condition of RTE.

8 Application to diffusiophoresis due to volume exclusion of a solute

To apply our framework, we focus on colloidal diffusion in the dilute limit, where analytical expressions of colloidal mobilities can be obtained based on a known fluid equation of state. Our framework predicts a novel contribution to phoretic motion arising solely from thermodynamic force disturbances $\delta\mathbf{X}$, in the absence of interfacial potential interactions. In general, such disturbances display a slower decay with distance

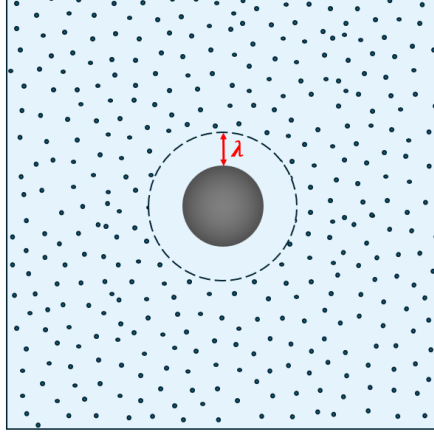


Figure 4: The excluded-volume interaction between the colloid and the solute leads to an interfacial excess layer around the colloid, containing solvent but void of solute particles.

than those due to interfacial potential interactions and can therefore not be considered directly within the BLA. This may explain why the corresponding contribution is often considered to be absent based on the assumption that the solvent can balance such disturbances,[15] which, however, does not align with the mechanism behind classical osmosis discussed earlier.

To demonstrate that such disturbances produce a convergent contribution to the colloidal diffusion velocity, we consider the diffusiophoretic motion at constant temperature of a single colloid whose solid boundary is defined by its hydrodynamic radius R . The colloid is suspended in a solution composed of a single solvent component l and a single ideal solute component k . As shown in Fig. 4, we assume that the colloid specifically interacts with the solute via an excluded-volume potential $\phi_k = \infty$ within a range $r \leq R + \lambda$ and zero elsewhere, where λ is the thickness of the excluded-volume layer around the solid boundary of the colloid. Diffusiophoresis is caused by a difference in solute number density across \mathcal{V} , which produces an ideal solute diffusion flux $\mathbf{j}_k = -n_k^{\text{eq}} \nabla_T \hat{\mu}_k / \xi_k$, where ξ_k is the friction coefficient of a solute particle. Since colloidal diffusion is slow compared to solute diffusion, the solute continuity equation reduces to a diffusive steady-state condition given by $\nabla \cdot \mathbf{j}_k = 0$ inside the colloidal rest frame. Due to the excluded-volume interaction, the boundary condition of vanishing normal diffusion flux $\hat{\mathbf{r}} \cdot \mathbf{j}_k = 0$ applies at $r = R + \lambda$, which corresponds to the outer boundary of the excluded-volume layer. Furthermore, the solvent diffusion flux is fixed by $\mathbf{j}_l = -w_k \mathbf{j}_k / w_l$, implying that solvent diffusion and solute diffusion are driven by the same thermodynamic force $\nabla_T \hat{\mu}_k$, namely a gradient in solute chemical potential, which satisfies $\nabla_T^2 \hat{\mu}_k = 0$ outside the excluded-volume layer.

Noting that $\nabla_T \hat{\mu}_k$ must tend to a uniform bulk value of $\nabla_T \hat{\mu}_k^{\text{b}} = k_B T \nabla n_k^{\text{b}} / n_k^{\text{b|eq}}$ far away from the colloidal surface, solving $\nabla \cdot \mathbf{j}_k = 0$ yields $n_k^{\text{eq}} \nabla_T \hat{\mu}_k = [\mathbf{I} + (\mathbf{I} - 3\hat{\mathbf{r}}\hat{\mathbf{r}})(R + \lambda)^3 / (2r^3)] \cdot k_B T \nabla n_k^{\text{b}}$ for $r > R + \lambda$ and zero elsewhere. The phoretic force density $\mathcal{F}_{\text{ph}} = -\delta(n_k^{\text{eq}} \nabla_T \hat{\mu}_k)$ therefore takes the form

$$\mathcal{F}_{\text{ph}} = \begin{cases} -\frac{1}{2} \frac{(R + \lambda)^3}{r^3} (\mathbf{I} - 3\hat{\mathbf{r}}\hat{\mathbf{r}}) \cdot k_B T \nabla n_k^{\text{b}}, & r > R + \lambda, \\ k_B T \nabla n_k^{\text{b}}, & r \leq R + \lambda. \end{cases} \quad (54)$$

As $n_k^{\text{eq}} = n_k^{\text{b|eq}}$ and hence $\delta n_k^{\text{eq}} = 0$ for $r > R + \lambda$, the dipolar contribution to the phoretic force density outside

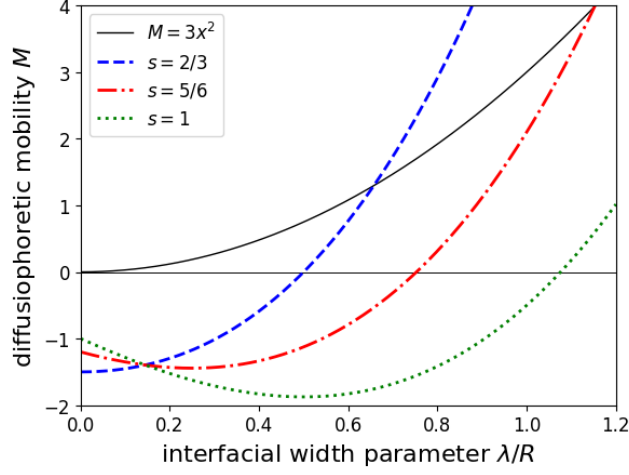


Figure 5: Rescaled diffusiophoretic mobility M of a single colloid due to volume exclusion of an ideal solute, plotted against the interfacial width parameter $x = \lambda/R$ for three different values of the hydrodynamic slip parameter s . The BLA applies for $x \ll 1$, whereas the Hückel limit applies for $x \gg 1$. For comparison, the classical result by Anderson[7] is shown by the black solid curve.

the excluded-volume layer stems entirely from a thermodynamic force disturbance $\nabla_T \delta \hat{\mu}_k$. In addition, we have $\phi_k = 0$ for $r > R + \lambda$, implying that outside the layer, the phoretic force density can be written as $\mathcal{F}_{\text{ph}} = -n_k^{\text{bleq}} \nabla_T \delta \hat{\mu}_k = -\nabla \delta \Pi$, where the local osmotic pressure Π simply coincides with the ideal osmotic pressure of the solute. We seek an explicit expression for the diffusiophoretic velocity \mathbf{v}_Δ , such that

$$\mathbf{v}_\Delta = -\frac{R^2}{9\eta} M k_B T \nabla n_k^{\text{b}}, \quad (55)$$

where M is the rescaled diffusiophoretic mobility of the colloid. In the absence of gravity and ciliary motion, Eq. (51) reduces to

$$\mathbf{v}_\Delta = \frac{1}{\xi_c} \int_{\tilde{\nu}} (\mathbf{U}_c^* - \mathbf{I}) \cdot \mathcal{F}_{\text{ph}} d^3 \mathbf{r}. \quad (56)$$

Using Eqs. (44), (45) and (54) in Eq. (56), and introducing the dimensionless interfacial width parameter $x = \lambda/R$, we find

$$M = \underbrace{\frac{x}{s} [2x^2 + 3(2-s)x + 6(1-s)]}_{M_\lambda} - \underbrace{\frac{1}{2s} (3sx^2 + 6sx + 2)}_{M_{\text{dif}}}. \quad (57)$$

If only the contribution M_λ from the excluded-volume layer is taken into account, then imposing a no-slip boundary condition ($s = 1$) and expanding this term to leading order in $x \ll 1$ gives $M = 3x^2$ and hence

$$\mathbf{v}_\Delta = -\frac{\lambda^2}{3\eta} k_B T \nabla n_k^{\text{b}}, \quad (58)$$

which precisely coincides with the result derived by Anderson in the BLA.[7] Eq. (57) therefore generalises this result to arbitrary layer thickness λ and hydrodynamic slippage s at the colloidal surface, while also

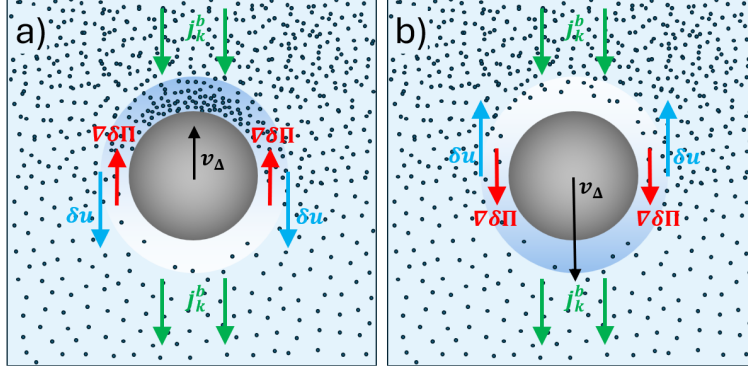


Figure 6: Diffusiophoresis of a single colloid due to a disturbance of the solute number density in the absence of an interfacial potential interaction. a) Diffusive polarisation across a passive colloid, resulting in a diffusiophoretic velocity given by Eq. (59). b) An active colloid with a perfectly absorbing surface, producing a diffusiophoretic velocity given by Eq. (60). The green, blue and red arrows show the average directions of the bulk solute flux \mathbf{j}_k^b , the induced osmotic pressure gradient $\nabla\delta\Pi$ and the induced fluid flow. The black arrows represent the diffusion velocity $\mathbf{v}_\Delta = \mathbf{v}_c - \langle \mathbf{u} \rangle$ of the colloid. The colour gradient around the colloidal surface is a schematic representation of $\delta\Pi$, with low values in white and high values in dark blue.

accounting for the contribution M_{dif} arising from the diffusive polarisation of solute particles outside the layer. Due to the latter contribution, the diffusiophoretic mobility M predicted by Eq. (57) differs considerably from Eq. (58). This is shown in Fig. 5, where M is plotted as a function of $x = \lambda/R$ for three different values of the hydrodynamic slip parameter s . Whereas Anderson's result exclusively predicts diffusiophoresis towards lower bulk solute concentration ($M = 3x^2 \geq 0$), Eq. (57) predicts the opposite trend for $x \ll 1$ over the entire range of hydrodynamic slippage $2/3 \leq s \leq 1$, while a crossover towards positive values of M eventually occurs at $x = 1/2$ for perfect slip ($s = 2/3$) and at $x \approx 1.08$ for no slip ($s = 1$).

Notably, the contribution M_{dif} persists at zero interfacial layer thickness ($x = 0$), giving $M = -1/s$ and thus

$$\mathbf{v}_\Delta = \frac{R^2}{9s\eta} k_B T \nabla n_k^b. \quad (59)$$

Eq. (59) predicts diffusiophoretic motion towards higher bulk solute concentration in the absence of interfacial potential interactions, as shown in Fig. 6a), with speeds of $\sim 0.1 - 1 \mu\text{m/s}$ based on typical parameter values. This behaviour can be understood intuitively: As the solute cannot diffuse through the colloid, it accumulates on the side of the colloid facing the bulk solute flux and depletes from the other side. The induced osmotic pressure gradient $\nabla\delta\Pi$ then drives a local fluid flow towards lower bulk solute concentration, while the colloid is pushed in the opposite direction. Under the same bulk condition, one may alternatively consider a chemically active colloid with a perfectly absorbing surface, by instead imposing the boundary condition $\Pi = 0$ at the colloidal surface, as shown in Fig. 6b). In this case, one has $\mathcal{F}_{\text{ph}} = (\mathbf{I} - 3\hat{\mathbf{r}}\hat{\mathbf{r}}) R^3/r^3 \cdot k_B T \nabla n_k^b$, which produces a diffusiophoretic velocity given by

$$\mathbf{v}_\Delta = -\frac{2R^2}{9s\eta} k_B T \nabla n_k^b, \quad (60)$$

corresponding to diffusiophoresis towards lower bulk solute concentration.

Finally, we recall that the trends shown in Fig. 5 are based on an excluded-volume potential, which may not always be realistic for modelling the solute distribution under repulsive interactions. For comparison, let us therefore reconsider the case of a passive colloid, but instead assume that the induced excess number density δn^{eq} is weak compared to the bulk density $n_k^{\text{b|eq}}$ and described by a smooth, long-ranged radial decay from the colloidal surface. In this case, the boundary condition of vanishing normal diffusion flux applies at $r \approx R$, and Eq. (56) can be written as[31]

$$\xi_c \mathbf{v}_\Delta = - \left(\int_{\tilde{v}} \frac{\delta n^{\text{eq}}}{n^{\text{b|eq}}} B d^3 \mathbf{r} - \frac{1}{2} \frac{4\pi R^3}{3} \right) k_B T \nabla n_k^{\text{b}}, \quad (61)$$

where the first term stems from the coupling of the excess solute number density δn^{eq} to the local chemical potential gradient $\nabla_T \hat{\mu}_k$, and the second term is due to the diffusive polarisation of solute around the colloid. The dimensionless function B depends on radial distance and is given by

$$B(r) = -1 + s \frac{R}{r} - \frac{1}{2} \left[\frac{s R^4}{2 r^4} + \left(1 - \frac{3s}{2} \right) \frac{R^6}{r^6} \right]. \quad (62)$$

For a net diffusiophoretic drift towards lower bulk solute concentration, the first term in Eq. (61) must dominate over the second term. A natural candidate for the solute excess profile is $\delta n^{\text{eq}} = -C n^{\text{b|eq}} R^4 / r^4$, since $1/r^4$ is the slowest integer-power decay yielding a finite solute excess, ensuring convergence of the volume integral in Eq. (61). The constant C quantifies the strength of the repulsive potential relative to the thermal energy $k_B T$ and must therefore satisfy $0 < C \lesssim 1$ for a weak disturbance of the solute number density. Using this profile to evaluate the first term in Eq. (61), one finds that diffusiophoresis occurs towards lower bulk solute concentration if $C > 35 / [9(25 - 13s)]$, which gives a maximal lower bound of $C \gtrsim 0.32$ for no slip ($s = 1$). This criterion suggests that "diffusiophobic" behaviour, namely diffusiophoretic motion towards lower bulk solute concentration, is indeed expected for longer-ranged and moderately repulsive interfacial interactions.

9 Conclusion

In general, resolving the local continuum dynamics in colloidal suspensions is theoretically and computationally demanding as it requires solving multiple coupled continuity equations under moving boundary conditions. As a result, existing approaches often rely on linear-response models that treat diffusive transport, including force-free phoretic motion, in a largely phenomenological manner.

Here, we have shown that this phenomenology can be reduced under kinematic reversibility by considering the hydrodynamics of colloidal sedimentation. In our continuum-statistical formulation, the Onsager reciprocal relations of colloidal transport arise naturally from the symmetry of the hydrodynamic response encoded in the Lorentz reciprocal theorem. Moreover, our framework consistently accounts for the solvent's response to momentum relaxation and fully resolves the coupling between thermodynamic forces and hydrodynamic flows beyond the boundary-layer approximation. As summarised in Fig. 7 for a single colloid, our approach decomposes into three independent and computationally tractable parts that represent the essential physical ingredients of a reciprocal treatment of colloidal diffusion: an equilibrium-statistical problem to determine the equation of state and local component distributions of the fluid (Fig. 7b)), a hydrodynamic problem to compute the auxiliary Stokes flow under stationary boundary conditions (Fig. 7d)), and a steady-state problem to determine the local thermodynamic forces (Fig. 7c)). The underlying linear-response assumption is not unduly restrictive, as fluxes are almost universally taken to be linear in the non-equilibrium forces

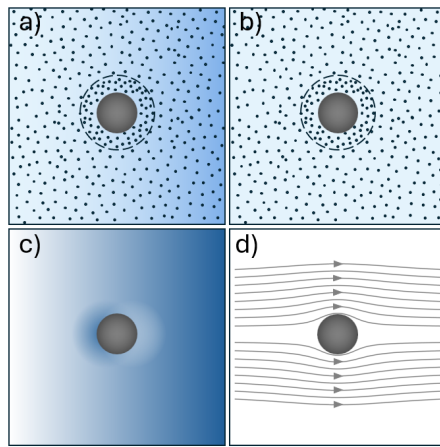


Figure 7: Schematic representation of the reciprocal approach to colloidal motion. a) A single colloid subjected to non-equilibrium forces. The continuum fields that these forces arise from are illustrated by a blue background gradient. The dashed circle around the colloid represents the effective boundary between its interfacial region and the bulk fluid. Instead of resolving the full local dynamics of a), the reciprocal approach consists of three alternative parts: b) An equilibrium-statistical problem to determine local component distributions, and a continuum-mechanical problem to independently compute c) the non-equilibrium forces and d) the induced Stokes flow field. A stronger background gradient is used in c) to show that the colloid can modify the continuum fields in its vicinity if the transport properties of its solid microphase differ from those of the solution.

in advection–diffusion problems. A natural and promising direction for future work is the numerical application of this approach to non-ideal osmotic equations of state, including solutes of finite size and colloidal concentrations beyond the dilute limit.

10 Acknowledgements

The author acknowledges helpful discussions with Daan Frenkel.

References

- [1] Sybren Ruurds De Groot and Peter Mazur. *Non-equilibrium thermodynamics*. Courier Corporation, 2013.
- [2] Lars Onsager. Reciprocal relations in irreversible processes. i. *Physical review*, 37(4):405, 1931.
- [3] Lars Onsager. Reciprocal relations in irreversible processes. ii. *Physical review*, 38(12):2265, 1931.
- [4] Nikolai V Churaev, Boris V Derjaguin, and Vladimir M Muller. *Surface forces*. Springer Science & Business Media, 2013.
- [5] J.N. Agar, Chung-Yuan Mou, and Jeong-Long Lin. Single-ion heat of transport in electrolyte solutions: a hydrodynamic theory. *The Journal of Physical Chemistry*, 93(5):2079–2082, 1989.
- [6] Jérôme Burelbach, Daan Frenkel, Ignacio Pagonabarraga, and Erika Eiser. A unified description of colloidal thermophoresis. *The European Physical Journal E*, 41(1):7, 2018.
- [7] John L Anderson. Colloid transport by interfacial forces. *Annual review of fluid mechanics*, 21(1):61–99, 1989.
- [8] Hassan Masoud and Howard A Stone. A reciprocal theorem for marangoni propulsion. *Journal of Fluid Mechanics*, 741:R4, 2014.
- [9] Jérôme Burelbach and Holger Stark. Linear and angular motion of self-diffusiophoretic janus particles. *Physical Review E*, 100(4):042612, 2019.
- [10] Max Teubner. The motion of charged colloidal particles in electric fields. *The Journal of Chemical Physics*, 76(11):5564–5573, 1982.
- [11] Thomas A Witten and Aaron Mowitz. Adapting the teubner reciprocal relations for stokeslet objects. *arXiv preprint arXiv:1907.07444*, 2019.
- [12] John F Brady. Phoretic motion in active matter. *Journal of Fluid Mechanics*, 922:A10, 2021.
- [13] Arkava Ganguly, Souradeep Roychowdhury, and Ankur Gupta. Unified mobility expressions for externally driven and self-phoretic propulsion of particles. *Journal of Fluid Mechanics*, 994:A2, 2024.
- [14] GK Batchelor. Brownian diffusion of particles with hydrodynamic interaction. *Journal of Fluid Mechanics*, 74(1):1–29, 1976.

- [15] John F Brady. Particle motion driven by solute gradients with application to autonomous motion: continuum and colloidal perspectives. *Journal of Fluid Mechanics*, 667:216–259, 2011.
- [16] Howard Brenner. Rheology of a dilute suspension of axisymmetric brownian particles. *International journal of multiphase flow*, 1(2):195–341, 1974.
- [17] W Yu and SUS Choi. The role of interfacial layers in the enhanced thermal conductivity of nanofluids: a renovated maxwell model. *Journal of nanoparticle research*, 5(1):167–171, 2003.
- [18] John Happel and Howard Brenner. *Low Reynolds number hydrodynamics: with special applications to particulate media*, volume 1. Springer Science & Business Media, 2012.
- [19] Hendrik Antoon Lorentz. Attempt of a theory of electrical and optical phenomena in moving bodies. *Versuch einer Theorie der Electricischen und Optischen Erscheinungen in Bewegten Körpern*. EJ Brill, 1895.
- [20] James R. Bielenberg and Howard Brenner. A continuum model of thermal transpiration. *Journal of Fluid Mechanics*, 546:1 – 23, 2005.
- [21] D Bedeaux, AM Albano, and P Mazur. Boundary conditions and non-equilibrium thermodynamics. *Physica A: Statistical Mechanics and its Applications*, 82(3):438–462, 1976.
- [22] Michael James Lighthill. On the squirming motion of nearly spherical deformable bodies through liquids at very small reynolds numbers. *Communications on pure and applied mathematics*, 5(2):109–118, 1952.
- [23] John R Blake. A spherical envelope approach to ciliary propulsion. *Journal of Fluid Mechanics*, 46(1):199–208, 1971.
- [24] GK Batchelor. The stress system in a suspension of force-free particles. *Journal of fluid mechanics*, 41(3):545–570, 1970.
- [25] Julien Morthomas and Alois Würger. Thermoelectric effect on charged colloids in the hückel limit. *The European Physical Journal E*, 27(4):425–434, 2008.
- [26] Benno Liebchen, Davide Marenduzzo, Ignacio Pagonabarraga, and Michael E Cates. Clustering and pattern formation in chemorepulsive active colloids. *Physical review letters*, 115(25):258301, 2015.
- [27] Howard A Stone and Aravinthan DT Samuel. Propulsion of microorganisms by surface distortions. *Physical review letters*, 77(19):4102, 1996.
- [28] Jan KG Dhont. Thermodiffusion of interacting colloids. i. a statistical thermodynamics approach. *The Journal of chemical physics*, 120(3):1632–1641, 2004.
- [29] Jérôme Burelbach, David B. Brückner, Daan Frenkel, and Erika Eiser. Thermophoretic forces on a mesoscopic scale. *Soft matter*, 14 36:7446–7454, 2018.
- [30] Jérôme Burelbach and Holger Stark. Determining phoretic mobilities with onsager’s reciprocal relations: Electro- and thermophoresis revisited. *The European Physical Journal E*, 42, 2018.
- [31] Jérôme Burelbach. Particle motion driven by non-uniform thermodynamic forces. *The Journal of chemical physics*, 150(14), 2019.